Microscopic and macroscopic models for the onset and progression of Alzheimer's disease

MICROSCOPIC AND MACROSCOPIC MODELS FOR THE ONSET AND PROGRESSION OF ALZHEIMER'S DISEASE

MICHIEL BERTSCH, BRUNO FRANCHI, MARIA CARLA TESI, AND ANDREA TOSIN

Abstract. In the first part of this paper we review a mathematical model for the onset and progression of Alzheimer's disease (AD) that was developed in subsequent steps over several years. The model is meant to describe the evolution of AD *in vivo*. In [1] we treated the problem at a microscopic scale, where the typical length scale is a multiple of the size of the soma of a single neuron. Subsequently, in [2] we concentrated on the macroscopic scale, where brain neurons are regarded as a continuous medium, structured by their degree of malfunctioning.

In the second part of the paper we consider the relation between the microscopic and the macroscopic models. In particular we show under which assumptions the kinetic transport equation, which in the macroscopic model governs the evolution of the probability measure for the degree of malfunctioning of neurons, can be derived from a particle-based setting.

The models are based on aggregation and diffusion equations for β-Amyloid (Aβ from now on), a protein fragment that healthy brains regularly produce and eliminate. In case of dementia Aβ monomers are no longer properly washed out and begin to coalesce forming eventually plaques. Two different mechanisms are assumed to be relevant for the temporal evolution of the disease: i) diffusion and agglomeration of soluble polymers of amyloid, produced by damaged neurons; ii) neuron-to-neuron prion-like transmission.

In the microscopic model we consider mechanism i), modelling it by a system of Smoluchowski equations for the amyloid concentration (describing the agglomeration phenomenon), with the addition of a diffusion term as well as of a source term on the neuronal membrane. At the macroscopic level instead we model processes i) and ii) by a system of Smoluchowski equations for the amyloid concentration, coupled to a kinetic-type transport equation for the distribution function of the degree of malfunctioning of the neurons. The transport equation contains an integral term describing the random onset of the disease as a jump process localized in particularly sensitive areas of the brain.

1. Introduction

The aim of the present paper is twofold: to provide an overview of the research carried on in the last few years by several authors in various collaborations on both microscopic and macroscopic mathematical models for Alzheimer's disease (AD) in the human brain [1, 2, 10, 11, 12], and to present a new result about the consistency of the microscopic and the macroscopic model. AD has a huge social and economic impact [4, 20, 23]. In 2015 it was estimated that about 44 million people suffered of AD, and until 2040 this number is expected to double every 20 years [35]. Not by chance AD-related issues belong to the cutting edge of scientific research. Apart from the classical *in vivo* and *in vitro* approaches, there is increasing interest in *in silico* research, based on mathematical modelling and computer simulations [6, 8, 13, 17, 18, 28, 41].

To cover the diverse facets of AD in a single model, different spatial and temporal scales must be taken into account: microscopic spatial scales to describe the role of the neurons, macroscopic spatial and short temporal (minutes, hours) scales for the description of the relevant diffusion processes in the brain, and large temporal scales (years, decades) for the description of the global development of AD. In [1, 12] the authors considered the problem at a microscopic scale, say a multiple of the size of the soma of a single neuron (from 4 to 100 μm). Subsequently, in [2] the authors introduced a macroscopic scale, treating brain neurons as a continuous medium and structuring them by their degree of malfunctioning. Mathematically, the bridge between the two models can be constructed in two different ways: by using either homogenisation theory (see [10, 11]) or modern Boltzmann-type kinetic theory for multi-agent systems. The latter approach will be developed in Section 4 of this paper.

Following closely the biomedical literature on AD, we briefly describe the processes (both microscopic and macroscopic) which we include in our models.

In the neurons and their interconnections several *microscopic phenomena* take place. It is largely accepted that beta amyloid (Aβ), especially its highly toxic oligomeric isoforms Aβ_{40} and Aβ_{42}, plays an important role in the process of the cerebral damage (the so-called *amyloid cascade hypothesis* [22]). In our papers we focus on the role of Aβ_{42} in its *soluble* form, which recently has been suggested to be the principal cause of neuronal death and eventually dementia [42]. Indeed techniques as enzyme-linked-immunosorbent assays (ELISAs) and mass spectrometry analysis suggest that the presence of plaques is not related to the severity of the AD. On the other hand, high levels of soluble Aβ correlate much better with the presence and degree of cognitive deficits than plaque statistics. As a matter of fact some authors (see for instance [16]) overturn the traditional perspective, claiming that large aggregates of Aβ can actually be inert or even protective to healthy neurons.

At the level of the neuronal membrane, monomeric Aβ peptides originate from the proteolytic cleavage of a transmembrane glycoprotein, the amyloid precursor protein (APP). By unknown and partially genetic reasons, some neurons present an unbalance between produced and cleared Aβ (we refer to such neurons as damaged neurons). In addition, it has been proposed that neuronal damage spreads in the neuronal net through a neuron-to-neuron prion-like propagation mechanism [5, 34].

On the other hand, *macroscopic phenomena* take place at the level of the cerebral tissue. The monomeric Aβ produced by damaged neurons diffuses through the microscopic tortuosity of the brain tissue and undergoes a process of agglomeration, leading eventually to the formation of long, insoluble amyloid fibrils, which accumulate in spherical deposits known as senile plaques. In addition, soluble Aβ shows a multiple neurotoxic effect: it induces a general inflammation that activates the microglia which in turn secretes proinflammatory innate cytokines [15] and, at the same time, increases intracellular calcium levels [13] yielding ultimately apoptosis and neuronal death.

The mathematical models which we derive in Sections 2 and 3 do not describe all the above-mentioned phenomena involved in the pathological process of AD. Actually there are several other phenomena which we neglect. For example, we do not consider the tortuosity of the brain tissue, we neglect the action of the τ-protein, we simplify the role of the microglia, and neglect its multifaceted mechanism. In fact, we simply assume that high levels of soluble amyloid are toxic for neurons at all scales. Our primary goal was to overcome the fundamental mathematical difficulties and set the basis for a highly flexible model, which can be easily fine-tuned to include other issues. On the other hand, when we work at macroscopic scale we take into account also a neuron-to-neuron prion-like propagation mechanism ([5, 34]).

The models are minimal but effective: the numerical simulations produce *a posteriori* images and graphs which are in good qualitative agreement with clinical findings and confirm the validity of our assumptions (see [2], and, in particular, Figg. 2–5). They also capture, at different scales, the cerebral damage in the early stage of the Mild Cognitive Impairment (MCI [33]).

In Section 4 we derive the equation for the progression of AD in the macroscopic model from a microscopic description of three main biophysical processes, among those recalled above. Namely, a prion-like spread of the disease over the neural network, the poisoning effect of soluble Aβ polymers diffusing in the brain tissue and stochastic jumps in the level of neuron malfunctioning due to uncontrolled causes, such as e.g. external agents or genetic factors. We use mathematical techniques coming from the modern Boltzmann-type kinetic theory for multi-agent systems [32], such as microscopic binary interaction schemes and mean-field asymptotic limits.

In Section 5 we highlight some shortcomings of the present approach and we discuss possible extensions of the models which could inspire future research directions.

2. Mathematical model at the microscopic scale

When aiming at producing mathematical models of biological phenomena we have to fix preliminarily a spatial scale, as well as a time scale. Thus, we consider a portion of the cerebral

cortex comparable in size to the size of a neuron, and we omit both the description of intracellular phenomena and clinical manifestations of the disease at a macroscopic scale, which will be considered instead in the model at the macroscopic scale. On the other hand, the experimental data of [24, 25] show that the process of plaques formation takes few days and therefore our temporal scale is chosen of the order of hours. In particular, no anatomical alteration of the neurons and of the surrounding cerebral tissue is taken into account.

The portion of cerebral tissue we consider is represented by a bounded smooth region $\Omega_0 \subset \mathbb{R}^3$ (or $\Omega_0 \subset \mathbb{R}^2$ in numerical simulations to reduce the computational complexity). To fix our ideas, we can think that the diameter of Ω_0 is of the order of 10 μm. This region contains several neurons; in the model the neurons are represented by a family of regular regions Ω_j such that (see Figure 1)

$\overline{\Omega}_j \subset \Omega_0$ if $j = 1, \dots, M$;
$\overline{\Omega}_i \cap \overline{\Omega}_j = \emptyset$ if $i \neq j$.

Here we denote by $\overline{\Omega}_j$ the closure of Ω_j, i.e. $\overline{\Omega}_j = \Omega_j \cup \partial\Omega_j$, where $\partial\Omega_j$ is the boundary of Ω_j. We set

$$\Omega := \Omega_0 \setminus \bigcup_{j=1}^{M} \overline{\Omega}_j.$$

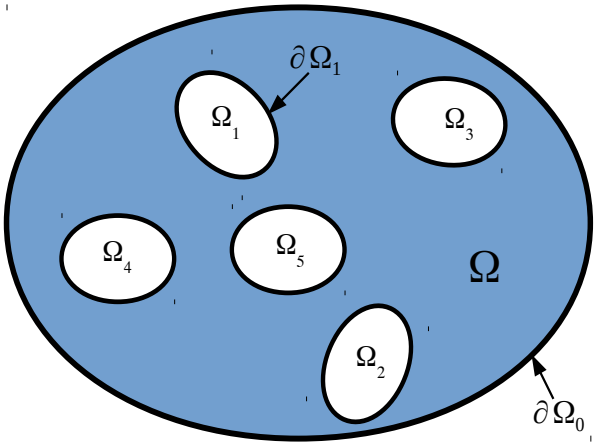

FIGURE 1. Schematic representation of a portion of the brain: the holes $\Omega_j, j = 1, \dots, 5$ represent neurons and $\partial\Omega_j$ their boundaries. Here $\overline{\Omega}_j = \Omega_j \cup \partial\Omega_j$, the dark region surrounding the holes is Ω, while $\Omega_0 = \Omega \cup \bigcup_{j=1}^{5} \overline{\Omega}_j$.

To describe the evolution of the amyloid in Ω, we consider a vector-valued function $u = (u_1, \dots, u_N)$, where $N \in \mathbb{N}$, $u_m = u_m(\tau, x)$, $m = 1, \dots, N$, $x \in \Omega$ is the space variable and $\tau \geq 0$ is the time variable. If $1 \leq m \leq N-1$ then $u_m(\tau, x)$ denotes the (molar) concentration at time $\tau \geq 0$ and point $x \in \Omega$ of Aβ assemblies of polymers of length m. In addition, u_N takes into account aggregations of more than $N-1$ monomers. Although u_N has a different meaning from the other u_m's, we keep the same letter u in order to avoid cumbersome notations. Clusters of oligomers of length $\geq N$ (fibrils) may be thought of as a medical parameter (the plaques), clinically observable through PIB-PET (Pittsburgh compound B - PET [30]).

Coherently with this choice of the scales, we assume that the diffusion of Aβ in Ω is uniform, and therefore employ the usual Fourier linear diffusion equation (see, for instance, [29]).

In addition, we describe the agglomeration phenomena by means of the so-called finite Smoluchowski system of equations with diffusion (of pure aggregation type). Classical references are [7, 37]; applications of Smoluchowski system to the description of the agglomeration of Aβ amyloid appeared for the first time in [28].

The production of Aβ in the monomeric form at the level of neuron membranes is modelled by a an inhomogeneous Neumann condition on $\partial\Omega_j$, the boundary of Ω_j, for $j = 1, \dots, M$. Finally, a homogeneous Neumann condition on $\partial\Omega_0$ is meant to neglect the neighbouring cerebral regions.

We are led to a coupled system, (1)-(2)-(3), of problems for u_m $(1 \le m \le N)$. u_1 satisfies the Cauchy-Neumann problem

$$
\begin{cases}
\partial_\tau u_1 = d_1 \Delta_x u_1 - u_1 \sum_{j=1}^{N} a_{1,j} u_j & \text{for } x \in \Omega,\ \tau > 0 \\
\partial_\nu u_1 = \psi_0 \equiv 0 & \text{for } x \in \partial\Omega_0,\ \tau > 0 \\
\partial_\nu u_1 = \psi_j & \text{for } x \in \partial\Omega_j,\ \tau > 0\ (j = 1, \dots, M) \\
u_1(x, 0) = U_1(x) \ge 0 & \text{for } x \in \Omega,
\end{cases} \tag{1}
$$

where $0 \le \psi_j \le 1$ is a smooth function for $j = 1, \dots, M$ which describes the production of the amyloid near the membrane of the neuron. We only take into account neurons affected by the disease, i.e. we assume $\psi_j \not\equiv 0$ for $j = 1, \dots, M$. Moreover, to avoid technicalities, we assume that U_1 is smooth, more precisely $U_1 \in \mathbf{C}^{2+\alpha}(\overline{\Omega})$ for some $\alpha \in (0, 1)$, and that $\partial_\nu U_1 = \psi_j$ on $\partial\Omega_j$, $j = 0, \dots, M$.

The Cauchy-Neumann problem for u_m $(1 < m < N)$ becomes

$$
\begin{cases}
\partial_\tau u_m = d_m \Delta_x u_m - u_m \sum_{j=1}^{N} a_{m,j} u_j + \frac{1}{2} \sum_{j=1}^{m-1} a_{j,m-j} u_j u_{m-j} & \text{for } x \in \Omega,\ \tau > 0 \\
\partial_\nu u_m = 0 & \text{for } x \in \partial\Omega,\ \tau > 0 \\
u_m(x, 0) = 0 & \text{for } x \in \Omega,
\end{cases} \tag{2}
$$

where $\partial\Omega = \partial\Omega_0 \cup \partial\Omega_1 \cup \cdots \cup \partial\Omega_M$, and u_N satisfies for all $x \in \Omega$ an ordinary differential equation:

$$
\begin{cases}
\partial_\tau u_N = \frac{1}{2} \sum_{\substack{j+k \ge N \\ k,\, j < N}} a_{j,k} u_j u_k & \text{for } x \in \Omega,\ \tau > 0 \\
u_N(x, 0) = 0 & \text{for } x \in \Omega.
\end{cases} \tag{3}
$$

Here $d_j > 0$ $(1 \le j < N)$ and $a_{i,j} = a_{j,i} > 0$ (for all subscripts i, j which occur).

We assume that the diffusion coefficients d_j are small when j is large, since big assemblies do not move. In fact, the diffusion coefficient of a soluble peptide scales approximately as the reciprocal of the cube root of its molecular weight (see [14, 29]). Plaques do not move, so if $m = N$ the equation does not contain a diffusion term.

The form of the coefficients $a_{i,j}$ (the coagulation rates) considered in [28, formula (13)] relies on sophisticated statistical mechanics considerations (see also [19, 39]). In our numerical simulations, we use a slightly approximate form of these coefficients, taking $a_{i,j} = \dfrac{C_{\text{aggr}}}{ij}$ where $C_{\text{aggr}} > 0$. In fact, this approximation basically consists in neglecting logarithmic terms in front of linear ones for large i, j. In the equation for u_N there is no term corresponding to the coefficient $a_{N,N}$; this is consistent with experimental data, since large oligomers do not aggregate with each other.

In our simulations we identify senile plaques with the sets $\{x \in \Omega : u_N(\tau, x) > c > 0\}$. Figure 2 represents a numerical implementation of the model (1), (2), (3). As in clinical observations, plaques grow near a neuron (the circle in Figure 2). The picture has been obtained by taking appropriate level sets of $u_N(\tau, \cdot)$.

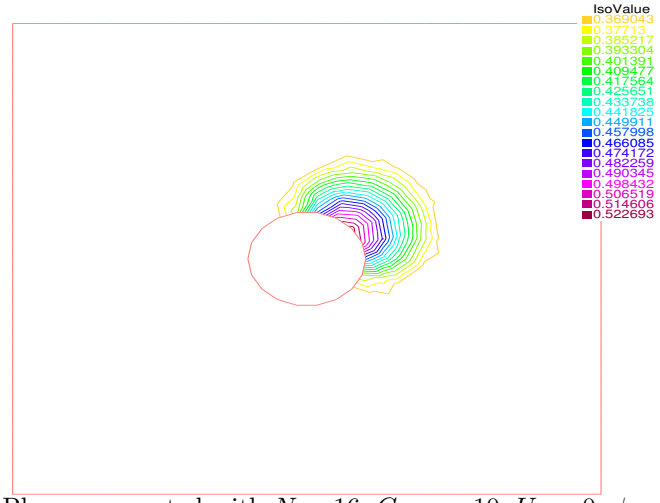

FIGURE 2. Plaque generated with $N = 16$, $C_{\text{aggr}} = 10$, $U_1 \equiv 0$, $\psi = 0.5$, $\tau = 40$. The curves in the picture represent the boundaries of the regions where $u_N(\tau, \cdot)$ exceeds the IsoValues of the same color. In addition, only the set $u_N > 0.3$ is presented, to show the shape of the senile plaque.

We notice that our model leads to a smooth shape of the senile plaques (because of standard regularity properties of diffusion equations), in disagreement with evidences found *in vivo*. This may be explained by Figure 3 in [8] and related comments on the role of the microglia.

Besides numerical simulations, the main result obtained in [1] for this model is the following existence theorem:

Theorem 2.1. *For all $T > 0$ the Neumann-Cauchy problem* (1), (2), (3) *has a unique classical positive solution $u \in \mathbf{C}^{1+\alpha/2,2+\alpha}([0,T] \times \overline{\Omega})$.*

To be precise we observe that in [1] this result was proved assuming that there is also a diffusion term in the equation for u_N (with small diffusivity) but the result can be easily extended to the case without diffusion of u_N.

3. Mathematical model at the macroscopic scale

We identify now a large portion of the cerebral tissue with a 3-dimensional region Ω, with diameter of Ω of the order of 10 cm. As for the time scale, a new phenomenon occurs: two temporal scales are needed to simulate the evolution of the disease over a period of years, i.e. besides the short (i.e., rapid) τ-scale (whose unit time coincides with hours) for the diffusion and agglomeration of Aβ [24] that we used for the microscopic model, we need a long (i.e., slow) t-scale (whose unit time coincides with several months) to take into account the progression of AD. We can write the relation between the two scales as $\Delta t = \varepsilon \Delta \tau$ for a small parameter $\varepsilon \ll 1$. Under this scaling the typical time, which is $O(1)$ in the τ-scale, becomes much shorter in the t-scale, precisely $O(\varepsilon)$.

At the macroscopic scale, the boundary vale problem for monomers (1) must have a different form. Indeed, the information given on the microscale by the non-homogeneous Neumann boundary condition is transferred into a source term $\mathcal{F}$ appearing in the macroscopic equation. This is due to the fact that at this scale neurons are reduced to points. Therefore, we have the following macroscopic equation for monomers:

$$\partial_\tau u_1 = d_1 \Delta_x u_1 - u_1 \sum_{j=1}^{N} a_{1,j} u_j + \mathcal{F} \tag{4}$$

while the equations in (2) and (3) remain unchanged.

Mathematically, the transition from system (1) to equation (4) has been obtained by a two-scale homogenisation procedure described in [10] and [11].

The source term $\mathcal{F}$ in (4) will depend on the health state of the neurons. We model the *degree of malfunctioning* of a neuron with a parameter a ranging from 0 to 1: a close to 0 stands for "the neuron is healthy" whereas a close to 1 for "the neuron is dead". This parameter, although introduced for the sake of mathematical modelling (see also [34]), can be compared with medical images from Fluorodeoxyglucose PET (FDG-PET [27]).

For fixed $x \in \Omega$ and $t \geq 0$, let $f(x, a, t)$ be a probability measure, supported in $[0, 1]$, that indicates the *fraction* of neurons close to x with degree of malfunctioning between a and $a + da$ at time t. From now on, we denote by $X_{[0,1]}$ the space of probability measures on $\mathbb{R}$ that are supported in $[0, 1]$.

Since Aβ monomers are produced by neurons and the production increases if neurons are damaged, we choose in (4)

$$\mathcal{F} = \mathcal{F}[f] = C_{\mathcal{F}} \int_0^1 (\mu_0 + a)(1 - a) df(x, a, t). \tag{5}$$

The small constant $\mu_0 > 0$ accounts for the physiologic Aβ production by healthy neurons, and the factor $1 - a$ for the fact that dead neurons do not produce amyloid. For an exhaustive account on the mechanisms of interaction between amyloid production and damage of the neurons see the excellent review [38].

The progression of AD occurs in the slow time scale t, over decades, and is determined by the *deterioration rate* $v = v(x, a, t)$ of the health state of the neurons through the continuity equation:

$$\partial_t f + \partial_a (f v[f]) = 0. \tag{6}$$

Here $v[f]$ indicates that the deterioration rate depends on f itself.

We assume that

$$v[f] = \int_0^1 \mathcal{G}(x, a, b)\, df(x, b, t) + \mathcal{S}(x, a, u_1(x, \tau), \dots, u_{N-1}(x, \tau)). \tag{7}$$

The notation $\mathcal{G}$ takes into account the spreading of the disease by proximity, while $\mathcal{S}$ models the action of toxic Aβ oligomers, ultimately leading to apoptosis. For instance, we can choose

$$\mathcal{G}(x, a, b) = C_{\mathcal{G}}\, \rho(x)(b - a)^+, \tag{8}$$

where $\rho(x)$ denotes the neuron density at the point x. In addition

$$\mathcal{S} = C_{\mathcal{S}}(1 - a)\left(\sum_{m=1}^{N-1} m u_m(x, \tau) - \overline{U} \right)^+. \tag{9}$$

The threshold $\overline{U} > 0$ indicates the minimal amount of toxic Aβ needed to damage neurons, assuming that the toxicity of soluble $A\beta$-polymers does not depend on m. In reality length dependence has been observed [31], but, to our best knowledge, quantitative data are only available for very short molecules (see [31, Table 2]). For long molecules any analytic expression would be arbitrary.

The fact that the neuron density ρ is independent of time could suggest that the progressive atrophy, due to neuronal death, is neglected. To avoid misunderstandings we stress that this is not the case, since ρ describes the *original* neuron density at the time $t = 0$ (the "anatomy"), and the evolution in time of the measure $f(x, \cdot, t)$ takes into account the neuronal loss (the "pathology").

At this point, we stress that equation (6), by its own nature, fails to describe the onset of the disease. To describe the onset of AD we assume that in small, randomly chosen parts of the cerebral tissue, concentrated for instance in the hippocampus, the degree of malfunctioning of neurons randomly jumps to higher values due to external agents or genetic factors. This leads to an additional term in the equation for f,

$$\partial_t f + \partial_a \left(f v[f] \right) = J[f],$$

where $J[f]$ is *a measure* defined by the following identity between measures

$$J[f] = \eta \left(\Big\{ \int_0^1 P(t,\, a_* \to a)\, df(x,\, a_*,\, t) \Big\} \mathcal{L}_a - f(x,\, a,\, t) \right) \chi(x,\, t). \tag{10}$$

Here $\mathcal{L}_a$ is the usual Lebesgue measure in $[0, 1]$ with respect to the variable a. Moreover, $P(t,\, a_* \to a)$ is the probability to jump from the state a_* to a state $a \in [0,\, 1]$ (obviously, $P(t,\, a_* \to a) = 0$ if $a < a_*$), $\chi(x,\, t)$ describes the random jump distribution, and η is the jump frequency. For instance we can choose

$$P(t,\, a_* \to a) \equiv P(a_* \to a) = \begin{cases} \dfrac{2}{1 - a_*} & \text{if } a_* \le a \le \dfrac{1 + a_*}{2} \\ 0 & \text{otherwise,} \end{cases} \tag{11}$$

and neglect randomness, taking $\chi(x,\, t) \equiv \chi(x)$, concentrated in the hippocampus.

In addition we stress that

$$\int_{[0,1]} dJ[f] = 0. \tag{12}$$

Finally, to model the phagocytic activity of the microglia as well as other bulk clearance processes [21], we add a term $-\sigma_m u_m$ in equations (1) and (2), where $\sigma_m > 0$. It is reasonable to assume that σ_m is inversely proportional to the length of corresponding oligomers.

We consider a transversal section (i.e. a horizontal planar section: see, e.g., Fig. 3) of the brain that can be compared with radiological imaging (see, e.g., [2, Fig. 1]). For the sake of simplicity we schematise the section of the brain as a bounded connected region $\Omega \subset \mathbb{R}^2$, with two inner disjoint "holes" representing the sections of the cerebral ventricles. Consistently, we assume that the boundary of Ω consists of two disjoint parts: an outer boundary $\partial\Omega_{\text{out}}$ and an inner boundary $\partial\Omega_{\text{in}}$, i.e. the boundary of the cerebral ventricles consisting of two disjoint closed simple curves.

Eventually, we are led to the system

$$\begin{cases} \partial_t f + \partial_a \left(f v[f] \right) = J[f] \\ \varepsilon \partial_t u_1 = d_1 \Delta_x u_1 - u_1 \sum\limits_{j=1}^{N} a_{1,j} u_j + \mathcal{F}[f] - \sigma_1 u_1 \\ \varepsilon \partial_t u_m = d_m \Delta_x u_m + \dfrac{1}{2} \sum\limits_{j=1}^{m-1} a_{j,m-j} u_j u_{m-j} \\ \qquad\qquad\qquad - u_m \sum\limits_{j=1}^{N} a_{m,j} u_j - \sigma_m u_m \qquad (2 \le m < N) \\ \varepsilon \partial_t u_N = \dfrac{1}{2} \sum\limits_{\substack{j+k \ge N \\ k,\, j < N}} a_{j,k} u_j u_k, \end{cases} \tag{13}$$

with τ replaced by $\varepsilon^{-1} t$. Since we are interested in longitudinal modelling, we assume that initially, at $t = 0$, there is a small uniform distribution of soluble amyloid $u_0 = (u_{0,1}, \dots, u_{0,N})$. In the equation for u_N there is no diffusion term since we assume that plaques are too big to diffuse, and the "degradation" term is omitted since we assume that the phagocytic activity of the microglia does not take place (since plaques are too big to be eaten, see Eq (2.16) in [2]).

Thus system (13) has to be coupled with Cauchy initial data

$$\begin{cases} f(x, a, 0) = f_0(x, a) & \text{if } x \in \Omega,\ 0 \le a \le 1 \\ u_i(x, 0) = u_{0,i}(x) & \text{if } x \in \Omega,\ 1 \le i \le N, \end{cases} \tag{14}$$

where the $u_{0,i} \in C^1(\overline{\Omega})$ are nonnegative functions for $i = 1, \dots, N$, and $f_0 \in L^\infty(\Omega; X_{[0,1]})$ describes the distribution of the disease at time $t = 0$.

On the outer boundary $\partial\Omega_{\text{out}}$ we assume vanishing normal polymer flow. Therefore we impose a homogeneous Neumann condition for the diffusing amyloid polymers:

$$-\frac{d_m}{\varepsilon} \Delta_x u_m \cdot \mathbf{n} = 0 \quad \text{on } \partial\Omega_{\text{out}}, \quad m = 1, \dots, N - 1, \tag{15}$$

$\mathbf{n}$ being the outward normal unit vector to $\partial\Omega_{\text{out}}$. Notice that no boundary condition is required for the concentration u_N of the fibrillar amyloid, since its equation does not feature space dynamics (cf. the last equation in (13)). On the inner boundary $\partial\Omega_{\text{in}}$, that is the boundaries of the cerebral ventricles, we model the removal of Aβ from cerebrospinal fluid (CSF) through the choroid plexus (cf. [21, 36]) by an outward polymer flow proportional to the concentration of the amyloid. For this, we impose a Robin boundary condition of the form:

$$-\frac{d_m}{\varepsilon}\Delta_x u_m \cdot \mathbf{n} = \gamma u_m \quad \text{on } \partial\Omega_{\text{in}}, \quad m = 1, \dots, N-1, \tag{16}$$

with $\gamma > 0$ a constant.

An existence and uniqueness theorem for system (13) with Cauchy initial data (14) and boundary conditions (15) and (16) is proved in [3]. With our choices of P, $\mathcal{G}$ and $\mathcal{S}$ in (11), (8) and (9), it reads as follows:

Theorem 3.1. *For all $T > 0$ there exist a unique $(N+1)$-ple*

$$(f, u_1, \cdots, u_N) \in L^\infty(\Omega;\, C([0,T];\, X_{[0,1]})) \times C((0,T];\, C^1(\overline{\Omega})^N),$$

$u_i \geq 0$ for $i = 1, \dots, N$, solving (13) *in a weak sense in $[0,T]$, with Cauchy data* (14) *and boundary data* (15) *and* (16)*.*

In particular, the first equation in (13) is satisfied in the following weak sense: for a.e. $x \in \Omega$, for $\phi = \phi(x, \cdot, \cdot) \in \mathcal{D}(\mathbb{R} \times [0,T])$ and for all $t \in [0,T]$

$$\int_0^t \left(\int (\partial_s \phi + v \partial_a \phi) df(x, \cdot, s) + \int \phi\, dJ(x, \cdot, s) \right) ds$$
$$= \int \phi(x, \cdot, t) df(x, \cdot, t) - \int \phi(x, \cdot, 0) df_0(x, \cdot).$$

Concerning the outputs of the numerical simulation of (13) with Cauchy initial data (14) and boundary conditions (15) and (16), it is instructive to compare plots of f, at different times, with FDG-PET images (see e.g. [9]): we create a schematic image of a transverse section of the brain and attribute different colors (varying from red to blue) to those parts of the brain where probabilistically the level of malfunctioning lies in different ranges. As in the FDG-PET, the red corresponds to a healthy tissue. Here AD originates only from the hippocampus and propagates, at the beginning, along privileged directions (such as those corresponding to denser neural bundles: see e.g. [34]) mimicked by two triangles. In the proposed model, this is simulated by assuming that the neuron density ρ is non-constant in x. In particular, ρ is supposed to attain its maximum value in two triangular-shaped regions connecting the hippocampus, namely the two circular regions of the domain, to the occipital part of the brain (the bottom edge of the domain), see Figures 3-5. From Eq. (7) one gets then that the higher ρ the higher is the neural deterioration rate due to the prion-like transmission (first term of the expression of $v[f]$), which finally results in a macroscopic directionality of the AD propagation.

Obviously the details of the numerical output depend on the choice of the constants used in the mathematical model. Performing a considerable amount of numerical runs with different values of the constants in the model, we have reached the conclusion that, at least qualitatively, the behaviour of the solutions does not depend on the precise choice of those constants, as long as their variation is restricted to reasonable ranges (i.e. within the same order of magnitude).

We report the values of the parameters we used in the numerical tests corresponding to Figures 3–5 in Table 1.

The constant γ enters the model through condition (16) at the boundary of the cerebral ventricles. Smaller values of γ mean that less Aβ is removed from the CSF through the choroid plexus. The comparison of the cases $\gamma = 1$ and $\gamma = 0.01$ becomes quite clear when we create spatial plots of f (taking into account the average degree of malfunctioning of the brain in every point) at fixed computational times $t = T$. In Figures 3 and 4, where we compare plots of f at, respectively, times $T = 30$ and $T = 40$ for the two different values of $\gamma = 0.01$ and $\gamma = 1$, AD originates only from the hippocampus and propagates, at the beginning, along privileged directions (such as those corresponding to denser neural bundles) mimicked by two triangles. Two remarks are

TABLE 1. Model parameters for the numerical tests of Section 3

Parameter	Reference	Figure 3	Figure 4	Figure 5
μ_0	Eq. (5)	0	0	0
$C_{\mathcal{F}}$	Eq. (5)	10^2	10^2	10^2
$C_{\mathcal{G}}$	Eq. (8)	10^{-1}	10^{-1}	10^{-1}
$C_{\mathcal{S}}$	Eq. (9)	$5 \cdot 10^{-2}$	$5 \cdot 10^{-2}$	$5 \cdot 10^{-2}$
$\overline{U}$	Eq. (9)	$5 \cdot 10^{-1}$	$5 \cdot 10^{-1}$	$5 \cdot 10^{-1}$
η	Eq. (10)	1	1	1, 1
N	Eq. (13)	3	3	3
d_m $(m = 1, \ldots, N-1)$	Eq. (13)	$10^{-2}/\sqrt[3]{m}$	$10^{-2}/\sqrt[3]{m}$	$10^{-2}/\sqrt[3]{m}$
σ_m $(m = 1, \ldots, N-1)$	Eq. (13)	$1/m$	$1/m$	$1/m$
ε	Eq. (13)	10^{-1}	10^{-1}	10^{-1}, 10^{-1}
γ	Eq. (16)	10^{-2}, 1	10^{-2}, 1	1
T	Final time	30	40	30, 60

now in order. First of all, though our images represent a *mean value* of brain activity instead of a single patient's brain activity, still they show a good agreement with clinical neuroimaging (obviously representing the specific situation of an individual patient). See, e.g. [26], reproduced also with permission in [2], Fig. 6. The specificities (both anatomic and physiologic) of the single patient might account for the discrepancies between the outputs of our simulations and clinical neuroimaging. Secondly, we notice that if γ becomes smaller (corresponding to a lower rate of clearance of the amyloid), we observe a temporal acceleration of the development of the illness; this could indicate the potential importance of the removal of $A\beta$ through the choroid plexus to slow down the temporal development of AD.

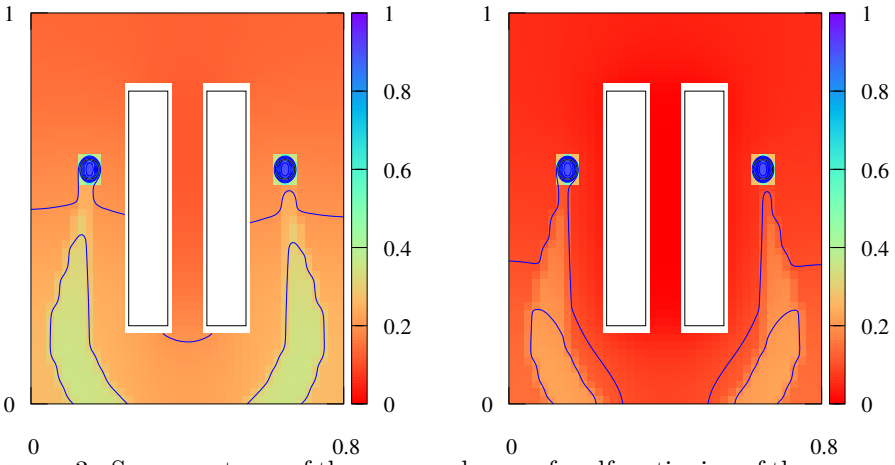

FIGURE 3. Space contours of the average degree of malfunctioning of the neurons, computed as $A(t, x) := \frac{1}{\rho(x)} \int_0^1 a f(t, x, a)\, da$, at time $T = 30$ with the sources of the disease concentrated in the hippocampus. The colour scale ranges from red, corresponding to fully healthy neurons, to blue, corresponding to dead neurons. The parameter γ entering the Robin boundary condition (16) is set to $\gamma = 10^{-2}$ in the left panel and to $\gamma = 1$ in the right panel. The latter case simulates a more abundant removal of Aβ through the choroid plexus with respect to the former case.

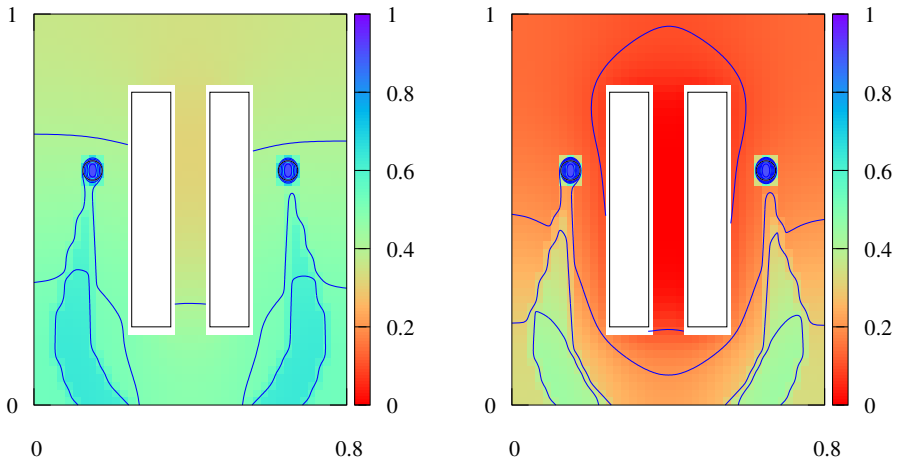

FIGURE 4. Continuation of the simulation shown in Figure 3 up to the time $T = 40$.

Looking for even more realistic images, we take now into account the randomness of the spatial distribution of the sources of the disease. Therefore we perform some runs where AD does not only originate from the hippocampus, but also from several sources of Aβ randomly distributed in the occipital part of the brain. We report the outputs of such runs, for $\gamma = 1$ and two different values of time T, in Figure 5. The randomly distributed sources appear as the small blue spots.

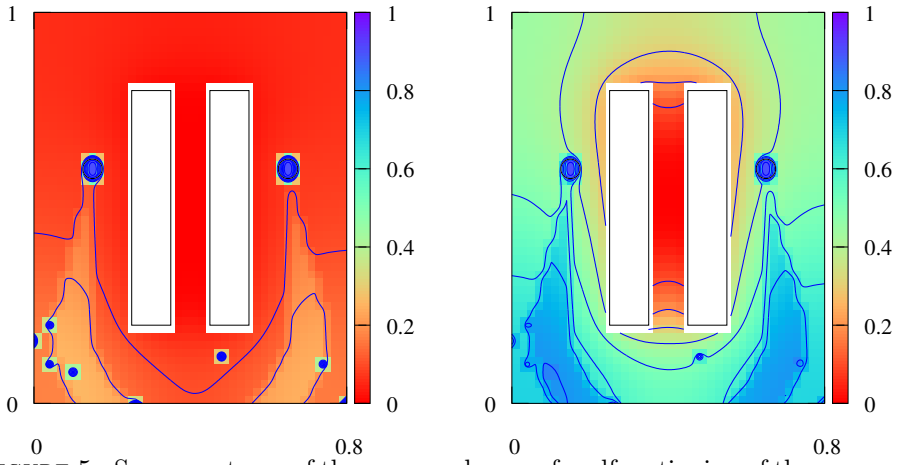

FIGURE 5. Space contours of the average degree of malfunctioning of the neurons, computed as $A(t, x) := \frac{1}{\rho(x)} \int_0^1 a f(t, x, a)\, da$, at times $T = 30$ (left panel) and $T = 60$ (right panel) with a random distribution of the sources of the disease. The colour scale ranges from red, corresponding to fully healthy neurons, to blue, corresponding to dead neurons.

Comparing the random sources case with the one in which AD originates only in the hippocampus, for the same values of $\gamma = 1$ and $T = 30$, it is clear that the brain sickness is more advanced when the number of sources is increased.

4. Derivation of the macroscopic equation for the progression of the disease

While the macroscopic system of Smoluchowski equations in (13) has been obtained from a smaller neuron-size scale through the homogenisation technique described in [10, 11], the mesoscopic equation for the distribution f of the disease has been so far postulated on a mainly heuristic

basis. In this section we provide its derivation from more fundamental particle-based dynamics, by adapting some arguments of the modern Boltzmann-type kinetic theory for multi-agent systems [32]. In this Section, for sake of simplicity, we assume that the probability measure $f(x, a, t)$ is absolutely continuous with respect to the Lebesgue measure $\mathcal{L}_a$, so that it can be written as the integral of a density that we can still denote by f.

4.1. **Binary interaction dynamics.** The derivation of a Boltzmann-type mesoscopic model relies strongly on the concept of *binary interactions* between pairs of neurons. This is the fundamental way in which microscopic dynamics among particles are described in the classical collisional kinetic theory. Here we revisit it in the non-strictly collisional framework of neuron-to-neuron interactions.

To begin with, we assume that the microscopic state of a single neuron is characterised by the pair $(X,\, A)$ in the state space $\Omega \times [0,\, 1]$, where $X \in \Omega$ is the position of the neuron in the brain and $A \in [0,\, 1]$ is its degree of malfunctioning. As such, the two microscopic variables X, A have to be regarded as independent of one another, in the sense that neither A is a function of X nor X is a function of A. On the other hand, in principle both evolve in time, thus $X = X(\tau)$ and $A = A(\tau)$ where $\tau \geq 0$ is the short (i.e. rapid) time variable as introduced in Section 3. As a matter of fact, since we do not consider any remodelling of the cerebral tissue over time, we can assume that X is constant in τ. Finally, in order to lighten the notation we set $A_\tau := A(\tau)$.

The idea of the binary interaction scheme mentioned above is that the time evolution of the microscopic state $(X,\, A_\tau)$ depends on repeated *individual* interactions with other neurons, each of which contributes to the variation of $(X,\, A_\tau)$ per unit of time. This is basically different from e.g. *mean field interactions*, also widely used in the microscopic modelling of interacting particle systems, which instead assume that the variation of $(X,\, A_\tau)$ in the unit time depends on the *average* of some *simultaneous* interactions with a certain number of other neurons. We anticipate that, as a result of the present derivation, we will obtain that mean field interactions are the macroscopically visible outcome for large times of the binary interactions taking place at short times.

An effective way of describing binary interactions is to consider a generic pair of neurons, say with microscopic states $(X,\, A_\tau)$, $(Y,\, B_\tau) \in \Omega \times [0,\, 1]$, respectively, and to model the individual action of the latter on the former. In doing so we appeal to the main biophysical mechanisms mentioned in the Introduction:

- A *neuron-to-neuron prion-like transmission* of the disease, which we model by a term of the form
$$K(X,\, Y,\, A_\tau,\, B_\tau) := \mathcal{G}(X,\, A_\tau,\, B_\tau) H_{X,Y},$$
where $\mathcal{G} : \Omega \times [0,\, 1] \times [0,\, 1] \to [0,\, 1]$ is a prescribed function which accounts for the prionic transmission of the disease and $H_{X,Y} \in \{0,\, 1\}$ is a variable which describes the structure of the neural network. Specifically, $H_{X,Y} = 1$ if the neurons in X and Y are connected by a synapse while $H_{X,Y} = 0$ if they are not.

  A possible form of the function $\mathcal{G}$ is $\mathcal{G}(X,\, A_\tau,\, B_\tau) \propto (B_\tau - A_\tau)^+$, cf. (8), meaning that the transmission of the disease depends on the relative degree of malfunctioning of the neurons involved in the binary interaction and is one-directional, namely from ill to healthier neurons only (in fact the proposed $\mathcal{G}$ is different from zero only if $B_\tau > A_\tau$). Notice that we do not exclude, in general, a possible dependence of $\mathcal{G}$ also on the position X of the attacked neuron. This is for the sake of generality, considering that the actual mechanisms of the prion-like transmission of AD are not yet fully understood at a clinical level. On the other hand, such a dependence does not cause any additional mathematical difficulty to the derivation of the model.

  In order to deal with the extremely complicated structure of the neural network, we consider a simple probabilistic description of it by assuming that $H_{X,Y}$ is a Bernoulli random variable parameterised by X, Y, in the sense that its law is
$$\mathbb{P}(H_{X,Y} = 1) = h(X,\, Y), \qquad \mathbb{P}(H_{X,Y} = 0) = 1 - h(X,\, Y) \tag{17}$$
for a given $h : \Omega \times \Omega \to [0,\, 1]$ such that $h(x,\, y) = h(y,\, x)$ for all $x,\, y \in \Omega$.

On the other hand, as an approximation we assume that the connections between neurons do not depend on time.

- The *poisoning effect of soluble $A\beta$ polymers* diffusing in the brain tissue, which we model by a function
$$\mathcal{S} = \mathcal{S}(X,\, A_\tau,\, u(X,\, \tau)),$$
where we have set $u(x,\, \tau) := (u_1(x,\, \tau),\, \dots,\, u_{N-1}(x,\, \tau))$, $x \in \Omega$, for brevity;
- *Stochastic jumps* in the degree of malfunctioning due to uncontrolled causes, such as external agents or genetic factors, which we model by means of a random variable J_τ such that
$$0 \leq J_\tau \leq 1 - A_\tau,$$
as in no case the new degree of malfunctioning after the jump, i.e. $A_\tau + J_\tau$, can be greater than 1.

In order to introduce a rule for the time variation of A_τ we assume that in a short time interval $\Delta\tau > 0$ there is a probability proportional to $\Delta\tau$ that the neuron undergoes any of the mechanisms mentioned above. Furthermore, we assume that each mechanism is independent of the others. A simple way to formalise this is to introduce three independent Bernoulli random variables T_ν, T_μ, $T_\eta \in \{0,\, 1\}$ such that

$$\mathbb{P}(T_\kappa = 1) = \kappa\Delta\tau, \quad \mathbb{P}(T_\kappa = 0) = 1 - \kappa\Delta\tau, \qquad \kappa = \nu,\, \mu,\, \eta,$$

where $\nu,\, \mu,\, \eta > 0$ are the frequencies associated to each of the mechanisms above while the time interval has to be chosen in such a way that $\Delta\tau < 1/\max\{\nu,\, \mu,\, \eta\}$. Under this assumption we set

$$A_{\tau+\Delta\tau} = A_\tau + T_\nu H_{X,Y}\mathcal{G}(X,\, A_\tau,\, B_\tau) + T_\mu\mathcal{S}(X,\, A_\tau,\, u(X,\, \tau)) + T_\eta J_\tau. \tag{18}$$

It is worth stressing that, unlike $H_{X,Y}$, $\mathcal{G}$, $\mathcal{S}$, J_τ, the variables T_ν, T_μ, T_η do not represent additional biological processes. Rather they translate the fact that any of the biological processes described by $H_{X,Y}$, $\mathcal{G}$, $\mathcal{S}$, J_τ may randomly happen in a time interval $\Delta\tau$.

4.2. **Boltzmann-type kinetic description.** Let $\varphi = \varphi(x,\, a) : \Omega \times [0,\, 1] \to \mathbb{R}$ be a test function representing any observable quantity that can be computed out of the microscopic state $(X,\, A_\tau)$ of a neuron. From (18) we get:

$$\varphi(X,\, A_{\tau+\Delta\tau}) = \varphi(X,\, A_\tau + T_\nu H_{X,Y}\mathcal{G}(X,\, A_\tau,\, B_\tau) + T_\mu\mathcal{S}(X,\, A_\tau,\, u(X,\, \tau)) + T_\eta J_\tau),$$

whence, averaging both sides and computing first the mean with respect to the variables T_ν, T_μ, T_η,

$$\begin{aligned}\langle\varphi(X,\, A_{\tau+\Delta\tau})\rangle = \langle\varphi(X,\, A_\tau)\rangle + \Delta\tau\Big[&\nu\,\langle\varphi(X,\, A_\tau + H_{X,Y}\mathcal{G}(X,\, A_\tau,\, B_\tau))\rangle\\ &+ \mu\,\langle\varphi(X,\, A_\tau + \mathcal{S}(X,\, A_\tau,\, u(X,\, \tau)))\rangle\\ &+ \eta\,\langle\varphi(X,\, A_\tau + J_\tau)\rangle\\ &- (\nu + \mu + \eta)\,\langle\varphi(X,\, A_\tau)\rangle\Big] + o(\Delta\tau),\end{aligned} \tag{19}$$

where $\langle\cdot\rangle$ denotes the average. Furthermore, using (17) to compute the mean with respect to $H_{X,Y}$ in the first term in brackets at the right-hand side, we obtain

$$\begin{aligned}&\langle\varphi(X,\, A_\tau + H_{X,Y}\mathcal{G}(X,\, A_\tau,\, B_\tau))\rangle\\ &\qquad = \langle\varphi(X,\, A_\tau + \mathcal{G}(X,\, A_\tau,\, B_\tau))h(X,\, Y)\rangle\\ &\qquad\quad + \langle\varphi(X,\, A_\tau)(1 - h(X,\, Y))\rangle\,,\end{aligned}$$

hence (19) specialises in

$$\begin{aligned}&\frac{\langle\varphi(X,\, A_{\tau+\Delta\tau})\rangle - \langle\varphi(X,\, A_\tau)\rangle}{\Delta\tau}\\ &\qquad = \nu\,\big\langle\big(\varphi(X,\, A_\tau + \mathcal{G}(X,\, A_\tau,\, B_\tau)) - \varphi(X,\, A_\tau)\big)h(X,\, Y)\big\rangle\\ &\qquad\quad + \mu\,\langle\varphi(X,\, A_\tau + \mathcal{S}(X,\, A_\tau,\, u(X,\, \tau)))\rangle\\ &\qquad\quad + \eta\,\langle\varphi(X,\, A_\tau + J_\tau)\rangle - (\mu + \eta)\,\langle\varphi(X,\, A_\tau)\rangle + o(1).\end{aligned}$$

In the limit $\Delta\tau \to 0^+$ this produces the continuous-in-time master equation

$$\begin{aligned}\frac{d}{d\tau}\langle\varphi(X,\,A_\tau)\rangle &= \nu\left\langle\big(\varphi(X,\,A_\tau+\mathcal{G}(X,\,A_\tau,\,B_\tau))-\varphi(X,\,A_\tau)\big)h(X,\,Y)\right\rangle\\ &\quad+\mu\left\langle\varphi(X,\,A_\tau+\mathcal{S}(X,\,A_\tau,\,u(X,\,\tau)))-\varphi(X,\,A_\tau)\right\rangle\\ &\quad+\eta\left\langle\varphi(X,\,A_\tau+J_\tau)-\varphi(X,\,A_\tau)\right\rangle.\end{aligned}\tag{20}$$

Let us now introduce the probability density function

$$g = g(x,\,a,\,\tau) : \Omega\times[0,\,1]\times\mathbb{R}_+ \to \mathbb{R}_+$$

of the microscopic state $(X,\,A_\tau)$, i.e. $g(x,\,a,\,\tau)\,dx\,da$ is the fraction of neurons which at time τ are in the infinitesimal volume dx centred at $x\in\Omega$ with a degree of malfunctioning in $[a,\,a+da]$. In the spirit of a *Boltzmann-type ansatz*, we assume that the processes $(X,\,A_\tau)$ and $(Y,\,B_\tau)$ are independent, so that their joint law is $g(x,\,a,\,\tau)g(y,\,b,\,\tau)$, cf. the next Remark 4.1. Moreover, we denote by $p(\tau,\,j|x,\,a)$, $0\le j\le 1-a$, the conditional law of J_τ with respect to $(X,\,A_\tau)$, which is such that

$$\int_0^{1-a} p(\tau,\,j|x,\,a)\,dj = 1,\qquad \forall\, x\in\Omega,\ a\in[0,\,1],\ \tau\ge 0.\tag{21}$$

The introduction of g and p makes it possible to average formula (20):

$$\begin{aligned}&\frac{d}{d\tau}\int_0^1\int_\Omega \varphi(x,\,a)g(x,\,a,\,\tau)\,dx\,da\\ &\qquad=\nu\int_0^1\int_0^1\int_\Omega\int_\Omega(\varphi(x,\,a^*)-\varphi(x,\,a))h(x,\,y)g(x,\,a,\,\tau)g(y,\,b,\,\tau)\,dx\,dy\,da\,db\\ &\qquad\quad+\mu\int_0^1\int_\Omega(\varphi(x,\,a^{**})-\varphi(x,\,a))g(x,\,a,\,\tau)\,dx\,da\\ &\qquad\quad+\eta\int_0^1\int_\Omega\int_0^{1-a}(\varphi(x,\,a^{***})-\varphi(x,\,a))p(\tau,\,j|x,\,a)g(x,\,a,\,\tau)\,dj\,dx\,da,\end{aligned}\tag{22}$$

where the starred variables denote the state of the neuron after one of the three types of interactions according to (20):

$$\begin{aligned}a^* &= a+\mathcal{G}(x,\,a,\,b) && \text{(prion-like transmission of the disease)}\\ a^{**} &= a+\mathcal{S}(x,\,a,\,u(x,\,\tau)) && \text{(poisoning by } A\beta \text{ polymers)}\\ a^{***} &= a+j && \text{(stochastic jumps).}\end{aligned}\tag{23}$$

Equations (22), (23) provide the *Boltzmann-type kinetic description* of the microscopic model formulated in Section 4.1.

Remark 4.1. Inspired by the discussion set forth in [32, Chapter 1], we observe that the assumption of stochastic independence of the states $(X,\,A_\tau)$, $(Y,\,B_\tau)$ is not fully justified from the biological point of view, being mostly dictated by the wish to obtain a closed equation in terms of the sole distribution function g. However, as it often happens in this type of problems, one needs to mediate between the high complexity of the biological phenomenon and the possibility to construct a usable, though necessarily approximated, mathematical model. In this respect, the aforesaid assumption should be regarded as a reasonable compromise, which permits a quite complete description and analysis of the evolution of the system.

4.3. **The quasi-invariant degree of malfunctioning limit.** As recalled in Section 3, the progression of AD occurs in a much slower time scale than that of the diffusion and agglomeration of Aβ polymers. This implies that the actual time scale where the macroscopic effects of the progression of AD are observable is much longer than the τ-scale at which the particle dynamics discussed in Sections 4.1, 4.2 take place. For this reason, as anticipated in Section 3 and inspired by the quasi-invariant interaction limits introduced in [32, 40], we now define the new time variable

$$t := \varepsilon\tau,\qquad 0<\varepsilon\ll 1,\tag{24}$$

where ε is a dimensionless parameter. Under this scaling, the typical time of a single particle transition (23), which is $O(1)$ in the τ-scale, becomes much shorter in the t-scale, precisely $O(\varepsilon)$. Simultaneously, we scale by ε also the interactions (23), considering that the effect of a single transition is attenuated in the longer t-scale. In particular, we set

$$\begin{aligned} a^* &= a + \varepsilon\,\mathcal{G}(x,\,a,\,b) \\ a^{**} &= a + \varepsilon\,\mathcal{S}(x,\,a,\,u(x,\,\tau)). \end{aligned} \tag{25}$$

As far as the stochastic jumps are concerned, we assume instead that the strength of a single jump is independent of the time scale, hence we still have $a^{***} = a + j$ also in the t-scale, but the frequency η of the jumps scales as $\varepsilon\eta$, i.e. single jumps are rarer, thus less probable, in the longer time scale.

In order to get from (22) an evolution equation in the t-scale, which avoids the detailed computation of the particle transitions in the unobservable τ-scale, we introduce the scaled distribution function

$$f(x,\,a,\,t) := g(x,\,a,\,t/\varepsilon),$$

which satisfies the relations $\int_0^1\int_\Omega f(x,\,a,\,t)\,dx\,da = 1$ and $\partial_t f = \frac{1}{\varepsilon}\partial_\tau g$, and, by (22), the equation

$$\begin{aligned} &\frac{d}{dt}\int_0^1\int_\Omega \varphi(x,\,a) f(x,\,a,\,t)\,dx\,da \\ &\quad= \frac{\nu}{\varepsilon}\int_0^1\int_0^1\int_\Omega\int_\Omega (\varphi(x,\,a^*) - \varphi(x,\,a)) h(x,\,y) f(x,\,a,\,t) f(y,\,b,\,t)\,dx\,dy\,da\,db \\ &\qquad+ \frac{\mu}{\varepsilon}\int_0^1\int_\Omega (\varphi(x,\,a^{**}) - \varphi(x,\,a)) f(x,\,a,\,t)\,dx\,da \\ &\qquad+ \eta\int_0^1\int_\Omega\int_0^{1-a} (\varphi(x,\,a^{***}) - \varphi(x,\,a)) P(t,\,j|x,\,a) f(x,\,a,\,t)\,dj\,dx\,da, \end{aligned} \tag{26}$$

where we have defined $P(t,\,j|x,\,a) := p(t/\varepsilon,\,j|x,\,a)$.

Taking $\varphi \in C^\infty(\Omega\times[0,\,1])$, with $\varphi(\cdot,\,0) = \varphi(\cdot,\,1) = 0$, we expand

$$\begin{aligned} \varphi(x,\,a^*) - \varphi(x,\,a) &= \varepsilon\partial_a\varphi(x,\,a)\mathcal{G}(x,\,a,\,b) + \frac{\varepsilon^2}{2}\partial_a^2\varphi(x,\,\tilde a)\mathcal{G}^2(x,\,a,\,b), \\ \varphi(x,\,a^{**}) - \varphi(x,\,a) &= \varepsilon\partial_a\varphi(x,\,a)\mathcal{S}(x,\,a,\,u(x,\,\tau)) + \frac{\varepsilon^2}{2}\partial_a^2\varphi(x,\,\bar a)\mathcal{S}^2(x,\,a,\,u(x,\,\tau)) \end{aligned}$$

with $\tilde a,\,\bar a \in (0,\,1)$, then we plug into (22) to get

$$\begin{aligned} &\frac{d}{dt}\int_0^1\int_\Omega \varphi(x,\,a) f(x,\,a,\,t)\,dx\,da \\ &\quad= \nu\int_0^1\int_0^1\int_\Omega\int_\Omega \partial_a\varphi(x,\,a)\mathcal{G}(x,\,a,\,b) h(x,\,y) f(x,\,a,\,t) f(y,\,b,\,t)\,dx\,dy\,da\,db \\ &\qquad+ \mu\int_0^1\int_\Omega \partial_a\varphi(x,\,a)\mathcal{S}(x,\,a,\,u(x,\,\tau)) f(x,\,a,\,t)\,dx\,da \\ &\qquad+ \eta\int_0^1\int_\Omega\int_0^{1-a} (\varphi(x,\,a^{***}) - \varphi(x,\,a)) P(t,\,j|x,\,a) f(x,\,a,\,t)\,dj\,dx\,da \\ &\qquad+ R(\varepsilon), \end{aligned}$$

where the remainder R is

$$\begin{aligned} R(\varepsilon) := &\frac{\nu\varepsilon}{2}\int_0^1\int_0^1\int_\Omega\int_\Omega \partial_a^2\varphi(x,\,\tilde a)\mathcal{G}^2(x,\,a,\,b) h(x,\,y) f(x,\,a,\,t) f(y,\,b,\,t)\,dx\,dy\,da\,db \\ &+ \frac{\mu\varepsilon}{2}\int_0^1\int_\Omega \partial_a^2\varphi(x,\,\bar a)\mathcal{S}^2(x,\,a,\,u(x,\,\tau)) f(x,\,a,\,t)\,dx\,da. \end{aligned}$$

Using that $0 \le h(x,\, y) \le 1$ and $\int_0^1 \int_\Omega f(x,\, a,\, t)\, dx\, da = 1$, we see that

$$|R(\varepsilon)| \le \frac{\varepsilon}{2} \left\|\partial_a^2 \varphi\right\|_\infty \left(\nu \left\|\mathcal{G}\right\|_\infty^2 + \mu \left\|\mathcal{S}\right\|_\infty^2\right).$$

Therefore, if $\mathcal{G}$ and $\mathcal{S}$ are bounded, $R(\varepsilon) \to 0$ as $\varepsilon \to 0^+$, and we obtain the equation

$$\begin{aligned} \frac{d}{dt} \int_0^1 \int_\Omega \varphi(x,\, a) f(x,\, a,\, t)\, dx\, da \\ = \int_0^1 \int_\Omega \partial_a \varphi(x,\, a) v[f,\, u](x,\, a) f(x,\, a,\, t)\, dx\, da \\ + \eta \int_0^1 \int_\Omega \int_0^{1-a} (\varphi(x,\, a^{***}) - \varphi(x,\, a)) P(t,\, j|x,\, a) f(x,\, a,\, t)\, dj\, dx\, da \end{aligned} \tag{27}$$

for

$$v[f,\, u](x,\, a) := \nu \int_0^1 \int_\Omega \mathcal{G}(x,\, a,\, b)\, h(x,\, y) f(y,\, b,\, t)\, dy\, db + \mu \mathcal{S}(x,\, a,\, u(x,\, \tau)). \tag{28}$$

Let us further inspect the last term at the right-hand side of (27). Substituting j with a^{***} according to (23) yields:

$$\begin{aligned} \int_0^1 \int_\Omega \int_0^{1-a} \varphi(x,\, a^{***}) P(t,\, j|x,\, a) f(x,\, a,\, t)\, dj\, dx\, da \\ = \int_0^1 \int_\Omega \int_a^1 \varphi(x,\, a^{***}) P(t,\, a^{***} - a|x,\, a) f(x,\, a,\, t)\, da^{***}\, dx\, da \end{aligned}$$

whence, switching the integrals in a^{***} and a,

$$= \int_0^1 \int_\Omega \varphi(x,\, a^{***}) \left(\int_0^{a^{***}} P(t,\, a^{***} - a|x,\, a) f(x,\, a,\, t)\, da \right) dx\, da^{***}.$$

On the whole (27) rewrites as

$$\begin{aligned} \frac{d}{dt} \int_0^1 \int_\Omega \varphi(x,\, a) f(x,\, a,\, t)\, dx\, da \\ = \int_0^1 \int_\Omega \partial_a \varphi(x,\, a) v[f,\, u](x,\, a) f(x,\, a,\, t)\, dx\, da \\ + \eta \int_0^1 \int_\Omega \varphi(x,\, a) \left(\int_0^a P(t,\, a - a_*|x,\, a_*) f(x,\, a_*,\, t)\, da_* - f(x,\, a,\, t) \right) dx\, da, \end{aligned}$$

which can be finally recognised as a weak form of

$$\partial_t f + \partial_a (f v[f,\, u]) = J[f].$$

This equation is a balance law with non-local transport velocity given by (28). The term $J[f]$ at the right-hand side is the *jump operator*

$$J[f](t,\, x,\, a) := \eta \left(\int_0^a P(t,\, a - a_*|x,\, a_*) f(\, x,\, a_*,\, t)\, da_* - f(x,\, a,\, t) \right),$$

which, owing to (21), is such that $\int_0^1 \int_\Omega J[f](t,\, x,\, a)\, dx\, da = 0$. Denoting the probability law of the jumps as $P(t,\, a_* \to a|x)$ we see that it is the term modelled in (10), with the dependence on the spatial distribution of the jumps hidden in the dependence of P on x.

Remark 4.2. If we assume that the neural network is composed by an extremely large number of neurons, which are connected mainly with other close neurons, we can take the probability h as $h(x,\, y) = \chi_{B_{1/N}(x)}(y)$, where N is the total number of neurons and $B_{1/N}(x) \subset \Omega \subset \mathbb{R}^n$ is the ball centred in the point x with radius $1/N$. If we suppose also $\nu \propto N^d$ (i.e. the more the neurons the

more frequent the prionic transmission of the disease among them) then in the limit $N \to \infty$ we obtain that $\nu h(x, y) \to \delta_0(y - x)$ and

$$v[f, u](x, a) = \int_0^1 \mathcal{G}(x, a, b) f(x, b, t)\, db + \mu \mathcal{S}(x, a, u(x, \tau)),$$

which is indeed the form of v postulated in (7).

Notice that, in general, v depends on contributions from multiple time scales, in fact the prionic transmission of the disease (first term at the right-hand side of the formula above) takes place in the slower t-scale while the poisoning of the neurons by Aβ polymers (second term at the right-hand side of the formula above) takes place in the faster τ-scale.

5. Discussion

There are two main features of our macroscopic model that deserve to be highlighted: first of all, as we showed above, it derives mathematically from a microscopic model we carefully developed relying on an accurately selected set of phenomena described in biomedical literature. This has been possible also thanks to the interdisciplinary character of our team, including mathematicians and medical doctors. Secondly, the model is characterised by a high level of flexibility, which potentially allows one to simulate different working hypotheses and compare them with clinical data. In fact, the model provides a flexible tool to test alternative conjectures on the evolution of the disease. Up to now we have chosen some specific aspects of the illness, such as aggregation, diffusion and removal of $A\beta$, possible spread of neuronal damage in the neural pathway, and, to describe the onset of AD, a random neural deterioration mechanism. Some mathematical results have been obtained, and numerical simulations have been compared with clinical data. Although we have restricted ourselves to a 2-dimensional rectangular section of the brain, the results are in good qualitative agreement with the spread of the illness in the brain at various stages of its evolution. In particular, the model captures the cerebral damage in the early stage of MCI.

There are several research issues that we would like to address in the future. As mentioned in the Introduction, the main shortcoming of the present model is the complete omission of the action of the τ protein and the microglia (in this context we mention a mathematical model proposed in [18]). The mechanisms related to the presence of the τ protein and the microglia should eventually be considered in a subsequent evolution of this model, both to obtain optimal quantitative agreement with clinical data and also to investigate the possible formation of patterns in the distribution of the level of malfunctioning of the brain.

From a numerical point of view, simulations should become more realistic, in a 3-dimensional domain which matches the geometric characteristics of the brain. Moreover, a certain sensitivity of the numerical output to the value of the constant γ in (16), which models the removal of $A\beta$ through the choroid plexus, spontaneously leads to the question whether dialysis-mechanisms can be introduced to enhance $A\beta$-removal artificially. Most probably, a serious answer to this question requires, in addition to a detailed comparison with clinical data, a more refined modelling of the clearance of soluble Aβ by the cerebral fluid.

In [1] and [2] the reader can find an exhaustive discussion of the literature on mathematical models for AD. Besides that, in the recent paper [17] a large system of reaction-diffusion equations is proposed as a macroscopic model which takes into account many of the processes which possibly play a role in the development of AD. In addition the paper contains some simulations of medical treatments. The authors do not consider the onset of AD, and model the action of the β-amyloid in a way which is quite different from our approach. In a forthcoming paper we shall compare both approaches.

Acknowledgments

This paper is dedicated to Stu with deep affection and gratitude.

The authors would like to express their gratitude to MD Norina Marcello for many stimulating and fruitful discussions over several years.

B. F. and M. C. T. are supported by the University of Bologna, funds for selected research topics, and by MAnET Marie Curie Initial Training Network. B. F. is supported by GNAMPA of INdAM (Istituto Nazionale di Alta Matematica "F. Severi"), Italy, and by PRIN of the MIUR, Italy.

A. T. is member of GNFM (Gruppo Nazionale per la Fisica Matematica) of INdAM (Istituto Nazionale di Alta Matematica "F. Severi"), Italy.

References

[1] Y. Achdou, B. Franchi, N. Marcello, and M. C. Tesi. A qualitative model for aggregation and diffusion of β-amyloid in Alzheimer's disease. *J. Math. Biol.*, 67(6-7):1369–1392, 2013.

[2] M. Bertsch, B. Franchi, N Marcello, M. C. Tesi, and A. Tosin. Alzheimer's disease: a mathematical model for onset and progression. *Mathematical Medicine and Biology*, 34:193–214, 2017.

[3] M. Bertsch, B. Franchi, M. C. Tesi, and A. Tosin. In preparation. (2017).

[4] K. Blennow, M. J. de Leon, and H. Zetterberg. Alzheimer's disease. *Lancet Neurol.*, 368:387–403, 2006.

[5] H. Braak and K. Del Tredici. Alzheimer's pathogenesis: is there neuron-to-neuron propagation? *Acta Neuropathol.*, 121(5):589–595, 2011.

[6] L. Cruz, B. Urbanc, S. V. Buldyrev, R. Christie, T. Gómez-Isla, S. Havlin, M. McNamara, H. E. Stanley, and B. T. Hyman. Aggregation and disaggregation of senile plaques in Alzheimer disease. *P. Natl. Acad. Sci. USA*, 94(14):7612–7616, 1997.

[7] R.L. Drake. A general mathematical survey of the coagulation equation. In *Topics in Current Aerosol Research (Part 2), International Reviews in Aerosol Physics and Chemistry*, pages 203–376. Pergamon Press, Oxford, UK, 1972.

[8] L. Edelstein-Keshet and A. Spiross. Exploring the formation of Alzheimer's disease senile plaques in silico. *J. Theor. Biol.*, 216(3):301–326, 2002.

[9] A. S. Fleisher, K. Chen, Y. T. Quiroz, L. J. Jakimovich, M. G. Gomez, C. M. Langois, J. B. S. Langbaum, N. Ayutyanont, A. Roontiva, P. Thiyyagura, W. Lee, H. Mo, L. Lopez, S. Moreno, N. Acosta-Baena, M. Giraldo, G. Garcia, R. A. Reiman, M. J. Huentelman, K. S. Kosik, P. N. Tariot, F. Lopera, and E. M. Reiman. Florbetapir PET analysis of amyloid-β deposition in the presenilin 1 E280A autosomal dominant Alzheimer's disease kindred: a cross-sectional study. *Lancet Neurol.*, 11(12):1057–1065, 2012.

[10] B. Franchi and S. Lorenzani. From a microscopic to a macroscopic model for Alzheimer disease: two-scale homogenization of the Smoluchowski equation in perforated domains. *J. Nonlinear Sci.*, 26(3):717–753, 2016.

[11] B. Franchi and S. Lorenzani. *Harmonic Analysis, Partial Differential Equations and Applications, In Honor of Richard L. Wheeden*, chapter Smoluchowski equation with variable coefficients in perforated domains: homogenization and applications to mathematical models in medicine, pages 49–68. Birkhäuser, 2017.

[12] B. Franchi and M. C. Tesi. A qualitative model for aggregation-fragmenattion and diffusion of β-amyloid in Alzheimer's disease. *Rend. Semin. Mat. Univ. Politec. Torino*, 7:75–84, 2012. Proceedings of the meeting "Forty years of Analysis in Torino, A conference in honor of Angelo Negro".

[13] T. A. Good and R. M. Murphy. Effect of β-amyloid block of the fast-inactivating K^+ channel on intracellular Ca^{2+} and excitability in a modeled neuron. *P. Natl. Acad. Sci. USA*, 93:15130–15135, 1996.

[14] G. J. Goodhill. Diffusion in axon guidance. *European Journal of Neuroscience*, 9(7):1414 – 1421, 1997.

[15] W. S. T. Griffin, J. G. Sheng, M. C. Royston, S. M. Gentleman, J. E. McKenzie, D. I. Graham, G. W. Roberts, and R. E. Mrak. Glial-neuronal interactions in Alzheimer's disease: the potential role of a cytokine cycle in disease progression. *Brain Pathol.*, 8(1):65–72, 1998.

[16] C. Haass and D. J. Selkoe. Soluble protein oligomers in neurodegeneration: lessons from the Alzheimer's amyloid beta-peptide. *Nat. Rev. Mol. Cell. Biol.*, 8(2):101–112, 2007.

[17] W. Hao and A. Friedman. Mathematical model on Alzheimer's disease. *BMC Systems Biology*, 108(10), 2016.

[18] M. Helal, E. Hingant, L. Pujo-Menjouet, and G. F. Webb. Alzheimer's disease: analysis of a mathematical model incorporating the role of prions. *J. Math. Biol.*, 69(5):1–29, 2013.

[19] T. L. Hill. Length dependence of rate constants for end-to-end association and dissociation of equilibrium linear aggregates. *Biophys J.*, 44:285–288, 1983.

[20] M. D. Hurd, P. Martorell, A. Delavande, K. J. Mullen, and K. M. Langa. Monetary costs of dementia in the United States. *New Engl. J. Med.*, 368(14):1326–1334, 2013.

[21] J. J. Iliff, M. Wang, Y. Liao, B. A. Plogg, W. Peng, G. A. Gundersen, H. Benveniste, G. E. Vates, R. Deane, S. A. Goldman, E. A. Nagelhus, and M. Nedergaard. A paravascular pathway facilitates CSF flow through the brain parenchyma and the clearance of interstitial solutes, including amyloid β. *Sci. Transl. Med.*, 4(147):147ra111, 2012.

[22] E. Karran, M. Mercken, and B. De Strooper. The amyloid cascade hypothesis for Alzheimer's disease: an appraisal for the development of therapeutics. *Nat Rev. Drug Discov.*, 10(9):698–712, 2011.

[23] M. P. Mattson. Pathways towards and away from Alzheimer's disease. *Nature*, 430:631–639, 2004.

[24] M. Meyer-Luehmann, T.L. Spires-Jones, C. Prada, M. Garcia-Alloza, A. De Calignon, A. Rozkalne, J. Koenigsknecht-Talboo, D. M. Holtzman, B. J. Bacskai, and B. T. Hyman. Rapid appearance and local toxicity of amyloid-β plaques in a mouse model of Alzheimer's disease. *Nature*, 451(7179):720–724, 2008.

[25] M. Meyer-Luhmann. *Experimental approaches to study cerebral amyloidosis in a transgenic mouse model of Alzheimer's disease*. PhD thesis, University of Basel, Faculty of Science, CH, 2004.
[26] J. C. Miller. Neuroimaging for dementia and Alzheimer's disease. *Radiology Rounds*, 4(4):1–4, 2006.
[27] L. Mosconi, V. Berti, L. Glodzik, A. Pupi, S. De Santi, and MJ. de Leon. Pre-clinical detection of Alzheimer's disease using FDG-PET, with or without amyloid imaging. *J. Alzheimer's Dis.*, 20(3):843–854, 2010.
[28] R. M. Murphy and M. M. Pallitto. Probing the kinetics of β-amyloid self-association. *J. Struct. Biol.*, 130(2-3):109–122, 2000.
[29] C. Nicholson and E. Sykov. Extracellular space structure revealed by diffusion analysis. *Trends in Neurosciences*, 21(5):207 – 215, 1998.
[30] A. Nordberg. Amyloid imaging in Alzheimer's disease. *Neuropsychologia*, 46(6):1636–1641, 2008.
[31] K. Ono, M. M. Condron, and D. B. Teplow. Structure-neurotoxicity relationships of amyloid β-protein oligomers. *P. Natl. Acad. Sci. USA*, 106(35):14745–14750, 2009.
[32] L. Pareschi and G. Toscani. *Interacting Multiagent Systems: Kinetic equations and Monte Carlo methods*. Oxford University Press, 2013.
[33] R. C. Petersen, R. O. Roberts, D. S. Knopman, B. F. Boeve, Y. E. Geda, R. J. Ivnik, G. E. Smith, and C. R. Jack Jr. Mild cognitive impairment: Ten years later. *Arch. Neurol.*, 66(12):1447–1455, 2009.
[34] A. Raj, A. Kuceyeski, and M. Weiner. A network diffusion model of disease progression in dementia. *Neuron*, 73(6):1204–1215, 2012.
[35] C. Reitz, C. Brayne, and R. Mayeux. Epidemiology of Alzheimer disease. *Nat. Rev. Neurol.*, 7:137–152, 2011.
[36] J.-M. Serot, J. Zmudka, and P. Jouanny. A possible role for CSF turnover and choroid plexus in the pathogenesis of late onset Alzheimer's disease. *J. Alzheimer's Dis.*, 30(1):17–26, 2012.
[37] M. Smoluchowski. Versuch einer mathematischen theorie der koagulationskinetik kolloider lsungen. *IZ. Phys. Chem.*, 92:129168, 1917.
[38] O. G. Tatarnikova, M. A. Orlov, and Bobkova N.V. Beta-amyloid and tau protein: Structure, interaction and prion-like properties. *Biochemistry (Moscow)*, 80(13):1800–1819, 2015.
[39] S. J. Tomsky and R. M. Murphy. Kinetics of aggregation of synthetic beta-amyloid peptide. *Arch. Biochem. Biophys.*, 294:630–638, 1992.
[40] G. Toscani. Kinetic models of opinion formation. *Commun. Math. Sci.*, 4(3):481–496, 2006.
[41] B. Urbanc, L. Cruz, S. V. Buldyrev, S. Havlin, M. C. Irizarry, H. E. Stanley, and B. T. Hyman. Dynamics of plaque formation in Alzheimer's disease. *Biophys. J.*, 76(3):1330–1334, 1999.
[42] D. M. Walsh and D. J. Selkoe. Aβ oligomers: a decade of discovery. *J. Neurochem.*, 101(5):1172–1184, 2007.

Dipartimento di Matematica, Università di Roma "Tor Vergata", Via della Ricerca Scientifica 1, 00133 Rome, Italy, and Istituto per le Applicazioni del Calcolo, CNR, Rome
E-mail address: bertsch@mat.uniroma2.it

Dipartimento di Matematica, Università di Bologna, Piazza di Porta San Donato 5, 40126 Bologna, Italy
E-mail address: bruno.franchi@unibo.it

Dipartimento di Matematica, Università di Bologna, Piazza di Porta San Donato 5, 40126 Bologna, Italy
E-mail address: mariacarla.tesi@unibo.it

Department of Mathematical Sciences "G. L. Lagrange", Politecnico di Torino, Corso Duca degli Abruzzi 24, 10129 Turin, Italy
E-mail address: andrea.tosin@polito.it